Iranian Journal of Geophysics, Vol 20 No 3, 2026, Page 153 – 165 (Research Article)
DOI: 10.30499/ijg.2025.508999.1678

A data-driven approach to reservoir characterization: machine learning and seismic Attribute integration in the penobscot field, Nova Scotia basin

Khlieeq Ul Zaman[1], Rani Ummay Farwa[1], Syed Haroon Ali[2*], Amjad Ali[3], Fahad Ali[4] and Muhammad Iqbal Hajana[5]

[1] *M.Sc student, Department of Earth Sciences, University of Sargodha, Pakistan*
[2] *Assistant Professor, Department of Earth Sciences, University of Sargodha, Pakistan*
[3] *Assistant Professor, College of Mechanical and Energy Engineering, Beijing University of Technology, Beijing, China*
[4] *Assistant Professor, Department of Geology, Bacha Khan University, Charsadda, Khyber Pakhtunkhwa, Pakistan*
[5] *Assistant Professor, Department of Earth and Environmental Sciences, Bahria University, Islamabad, Pakistan*

(Received: 18 May 2025, Accepted: 27 July 2025)

Abstract

Petrophysical analysis and advanced attributes of machine learning are used to evaluate exploratory wells, B-41 and L-30 of Penobscot Basin, Nova Scotia, Canada. The main objective of this paper is to evaluate the petroleum system and the prospects and leads. Well B-41 and L-30 reached their TD at 3483m and 4360m respectively, both wells were declared dry and plugged abandoned. The petrophysical studies include Bulk density and neutron porosity cross plots, in both wells, neutron and porosity cross plots show the almost linear trend of values, showing clay and sand lithology. Porosity values of B-41 and L-30 are 8-10% and 10-12%, respectively. Shale volume of B-41 is 37-44% and for L-30 is 23-32%; however, both wells show a fair porosity, but water saturation is high, so it is not a favorable condition for hydrocarbons to accumulate. For using attributes of machine learning 11 sets of 2D seismic lines and 1 set of 3D seismic surveys were used an advance technique of machine learning known as SOM (Self Organizing Map) is used, which is computational data analysis technique which enables mapping of nonlinear data to lower dimension and also at different frequencies, for this analysis the frequencies of 11, 18, 26 Hz are used. Machine learning enables efficient and accurate predictions even with limited data, providing a more practical and streamlined alternative to conventional reservoir simulation techniques.

Keywords: Petrophysical analysis, self-organizing map, dry well analysis, computational data analysis, hydrocarbon evaluation

*Corresponding author: haroon.ali@uos.edu.pk

1 Introduction

Penobscot, Nova Scotia, is between the Sable and Abenaki Sub-basins in Canada. It formed due to the breakup of the North American and African plates during rifting (Gibling et al., 2019). It is classified as an extensional basin, a geologically complex area having several major and minor faults. On the other side of the Atlantic, the Morocco basin is present and has the same characteristics as Penobscot (Pant et al., 2022). However, there are no discoveries from the Penobscot Basin, Nova Scotia. This is an extensional basin located in Nova Scotia, Canada (Narayan et al., 2023). This basin results from the rifting of the African and North American plates (Kroner et al., 2022). Penobscot Basin is a geologically complex basin, containing many minor and major faults (Campbell et al., 2015; Adim et al., 2018). This study's main steps and analysis are to facilitate the exploration of hydrocarbon resources by performing thorough geological and geophysical research. This involves assessing the petroleum system, paying particular attention to the integrity of the source, reservoir, seal, and trap (Moosavi et al., 2024; Mehrabi et al., 2024; Rafei et al., 2021). Finding and evaluating leads and prospects through integrated data interpretation is a primary objective. The study is to create ideas for additional exploratory activities based on the findings, guaranteeing data-driven and financially feasible decision-making for hydrocarbon exploration and development (Jelvegarfilband et al., 2022; Moosavi et al., 2023).

There have been no commercial oil or gas discoveries in the Penobscot basin. However, the Penobscot Basin has the potential to be a petroleum system that can produce (Wach & Brown, 2021). This study uses well log interpretation, seismic data analysis by using seismic attributes and machine learning (Mehrabi et al., 2025b) techniques like structural smoothing, ant tracking to identify the potential prospects. This study used 1 x 3D and 11 x 2D seismic lines. Location of the Penobscot is shown on the left side of Figure 1, and 11 2D seismic lines are shown on the right side of Figure 1.

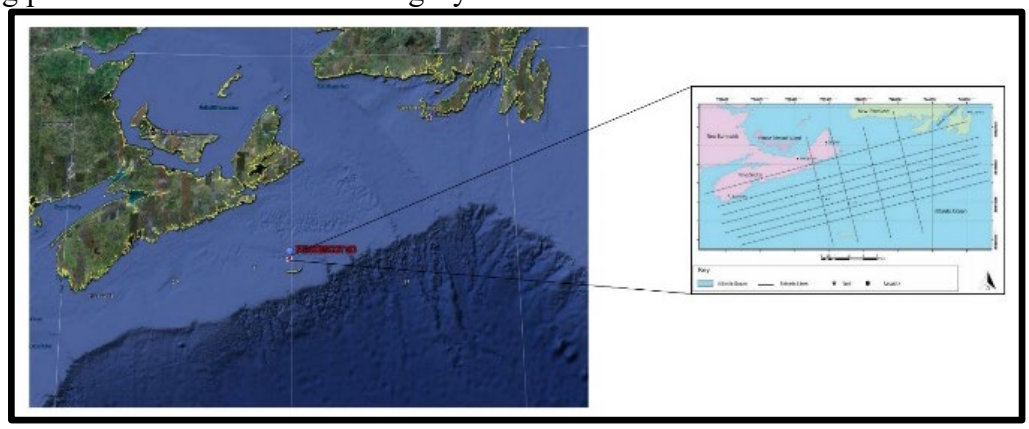

Figure 1. Showing Penobscot location on the left side with a white rectangular area and 11 x 2D seismic lines on the right side.

2 Methods and Data

In order to accomplish this study, basin modeling features, including porosity vs. depth curves (Mehrabi et al., 2025a), Vitrinite Reflectance vs. depth curves, and burial plots, are all done within basin modeling software. An industry-standardized software used for well log interpretation and correlation (Bashir et al., 2024; Olutoki et al., 2024).

Advanced industrial software is used for

seismic interpretation. In this phase, we carry out key activities to enhance seismic interpretation, including frequency feature integration for better stratigraphic resolution, Well to Seismic Tie for accurate depth correlation, Structural Smoothing to refine fault geometry, Ant Tracking and 3D Variance Analysis for detecting discontinuities, Data Conditioning to improve quality, and Horizon Definition for mapping geological boundaries. These results directly support reliable subsurface modeling and reservoir characterization (Abid et al., 2025; Ali et al., 2018; Ali et al., 2022). Well-to-seismic tie, structural smoothing, and ant tracking techniques were applied to identify faults and reduce noise in the data, thereby enhancing the clarity and reliability of the interpretation results. The relative geological time (RGT) model is also used in this study to understand subsurface dynamics better. This multidisciplinary study allows for a good and varied analysis of our area's geological features and characteristics. The workflow used in this article is shown in Figure 2.

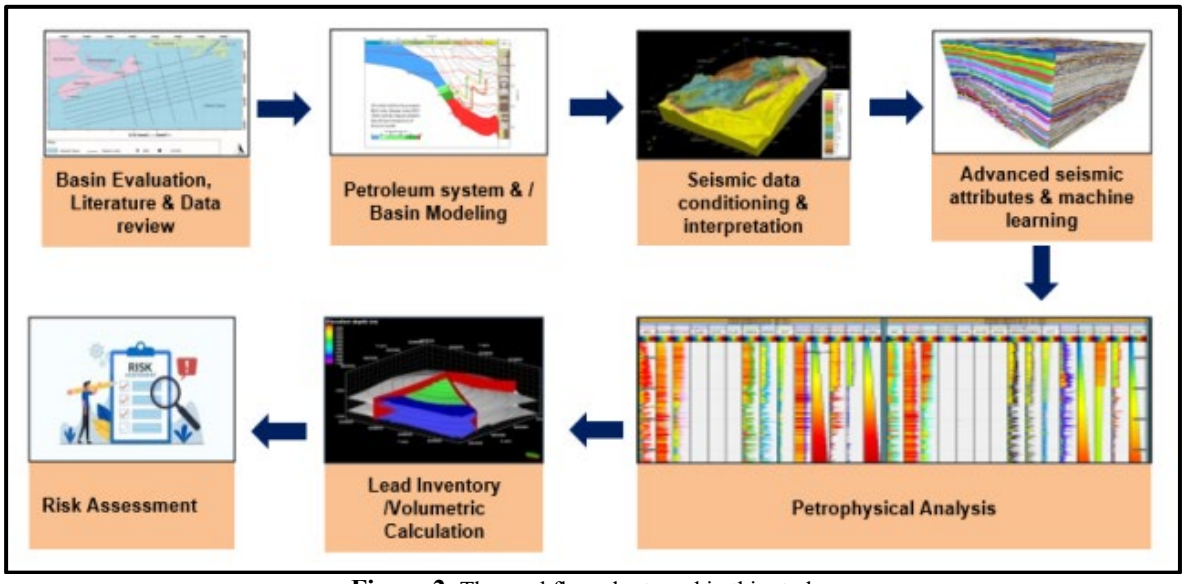

Figure 2. The workflow chart used in this study.

3 Objectives

Our study focused on the following objectives:

- A comprehensive geological and geophysical analysis to better understand subsurface structures and formations.
- Evaluation of the petroleum system, focusing on source rocks, reservoirs, and migration pathways.
- Identify and assess potential prospects and leads within the target area.
- A detailed proposal for further exploration outlines strategies for optimizing hydrocarbon discovery and extraction.

4 Structural Setup of Study Area

This region experienced multiple tectonic events during the Paleozoic Era, including the collision of continents, the formation of mountain ranges (orogenies), and periods of uplift and erosion (Fyffe et al., 2011). Due to this, folding produced that ranges from gentle to prominent folds (Robinson et al., 1998). The study area shows the complex setting of the area in which numerous anticline folds are shown in Figure 3 (Campbell, 2014). Faults are also present in this area. This area is dominated by an ENE-WSW fault set (Peace et al., 2024). Southward dipping faults are slightly more common than northward

dipping faults (Pharaoh et al., 2020). All smaller faults in the area are normal (Omeru et al., 2019).

Salt deposition occurred in this area during the Jurassic Period of the Mesozoic era (Pollock et al., 2012). Salt is present in the region below the inverted interval, and other structures were inverted by Salt flow.

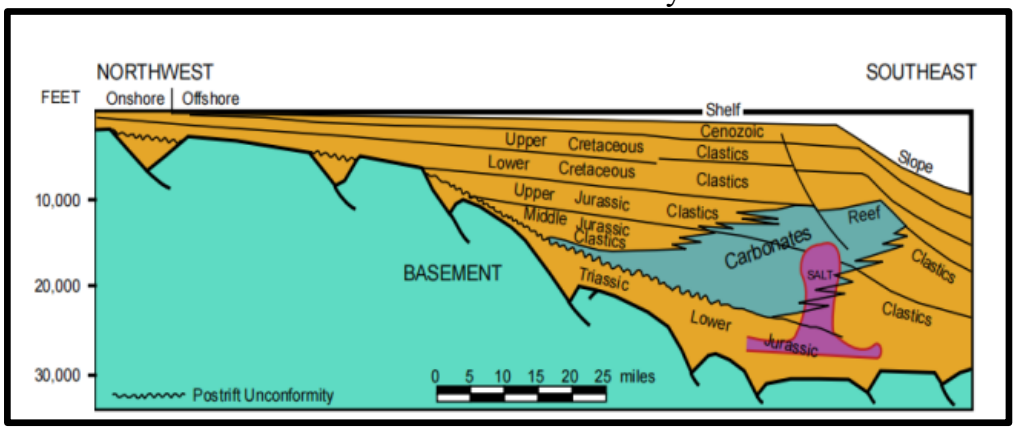

Figure 3. The Structural Setup of the Area and Salt Presence in the Area.

4.1 Stratigraphic Framework

The Stratigraphic Framework of Nova Scotia describes the layering of rocks deposited over millions of years. The ages of the rocks range from the Triassic to the Neogene, spanning from about 252 million years ago to the present day (Piper et al., 2011). The framework can be broadly divided into three tectonic settings:

The Pre-rift (~Triassic) period is characterized by deep to shallow marine environments, with red beds (sandstone, siltstone) and evaporates (salt deposits) deposited as the first infill of the basin (Saw et al., 2017; Omeru et al., 2019).

In the Syn-rift (~Early Jurassic), the continent rifted apart, deposited shallow marine clastic sediments (sandstone, shale) (Campbell et al., 2015; Mirza et al., 2024).

At the time of the Post-rift (~Middle Jurassic to Neogene), a major transgression (sea level rise) occurred, leading to the deposition of thick carbonate sequences (limestone, dolostone) throughout the Middle to Late Jurassic (Campbell, 2018; Ghazi et al., 2024). The Cretaceous period witnessed regression (sea level fall) with shallow marine environments (Eliuk, 1978). The remainder of the Mesozoic Era and the Cenozoic Era (Paleogene and Neogene) saw a mix of shallow marine and fluvial-deltaic (rivers and deltas) depositional environments (Mixon et al., 2000). Figure 4 shows the detailed stratigraphic column of the area and source presence.

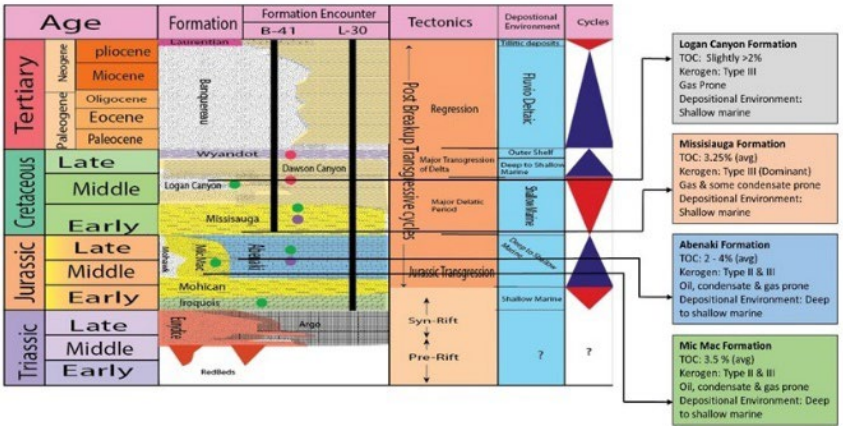

Figure 4. The stratigraphic column, the source rock presence, and its quality evaluatio

5 Results

5.1 Petrophysical Analysis

In our petrophysical synthesis, we have evaluated the main results of this study. The study showed hydrocarbon potential at an average depth of 3400 feet, which is the main target for this study. The main focus of the Petrophysical analysis is to evaluate the hydrocarbon potential and porosity of both wells.

In the petrophysical analysis, we evaluated the hydrocarbon potential and reservoir properties in both wells. The process began with reviewing and correcting the log data for any tool or measurement-related issues to ensure data reliability. This included checking for depth mismatches, removing spurious values, and ensuring consistency across logs. The gamma ray (GR) log was normalized to eliminate tool-related and regional variations, allowing for accurate lithological interpretation. Porosity was calculated using both density and neutron logs, and cross-plots were used to distinguish between clean and shaly formations. Water saturation was estimated using resistivity logs in combination with porosity data, applying standard models to identify hydrocarbon-bearing zones. Lithology was interpreted by integrating GR, density, neutron, and resistivity logs, which helped in classifying different rock types within the formation. By combining the results of porosity, saturation, and lithology analyses, we were able to identify and evaluate the intervals with significant hydrocarbon potential, aiding in the assessment of reservoir quality and exploration prospects.

It is important to mention that in addition to the hydrocarbon potential, the analysis shows no porosity in the two wells. This result indicates problems related to the quality of the assets in this area. The presence of hydrocarbons at this depth indicates the complexity of the subsurface geology in the area. To overcome the limitations of the low porosity, new extraction strategies may be required (Abid and Ali, 2024). Figures 5 and 6 show the petrophysical interpretation of Well L-30 and B-41, respectively.

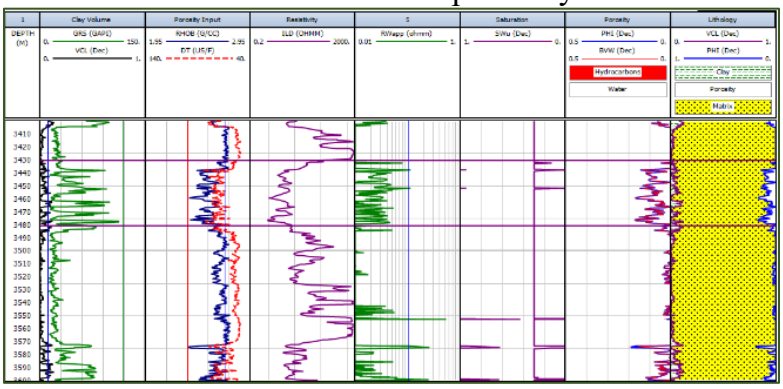

Figure 5. The Petrophysical Interpretation of Well L-30.

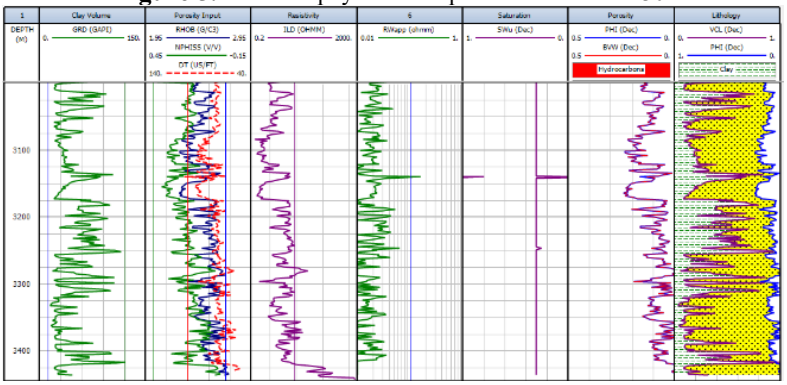

Figure 6. The Petrophysical Interpretation of Well B-41.

5.2 Petrophysical Interpretation

The process of combining petrological data with physical measurements of rocks is called petrophysical analysis (Dentith et al., 2020). Typically, well lithography is interpreted using wireline logs such as gamma ray (GR), bulk density (RHOB), deep resistivity (LLD), surface resistivity (LLS), neutron porosity (NHPI) and sonic (DT). For this paper, the lithology of both wells is interpreted by a combination of wireline logs (GR, RHOB, NPHI, DT, and LLD). The natural gamma ray log is the best indicator and differentiator between clay minerals and clean sands. Higher values of gamma rays indicate a high concentration of clay content, decreasing the effective permeability and porosity of the formation interval (Ahmed et al., 2025). In this research, the sandstone is the dominant lithology in the permeable formation interval. Higher values of gamma ray, neutron log, and density log suggest shale portion, but a sudden increase in the resistivity values is due to no water content, due to diagenetic processes like cementation and compaction.

5.3 Shale Volume Calculation

For this purpose, Dolan's method is used by using the GR log. The gamma ray index is given below

GRI: GR log – Gr min ÷ GR max – GR min

GR log is the gamma ray reading of formation, GR min is the minimum value of gamma ray, and GR max is the maximum value of gamma ray. The values of clean sands range from (2-130 API, and for shale, values range from (140-250) API. The shale content varies in different zones, especially in B-41 from 3100m to 3400m.

5.4 Porosity Calculation

Estimating porosity can be carried out by combining the density log and neutron log.

5.4.1 Total Porosity

The following equation can calculate the total porosity

$$\phi = \frac{\phi_{\log} - V_{sh} \cdot \phi_{sh}}{1 - V_{sh}}$$

Where:

- ϕ = corrected (effective) porosity
- ϕlog = total porosity from logs (e.g., density or neutron)
- V_{sh} = volume of shale (from GR or other logs)
- ϕ_{sh} = porosity of shale (usually ~0.10–0.15, depending on region)

The following equation calculates the density porosity

$\Phi D = (\rho ma - \rho b) / (\rho ma - \rho f)$,

where ρb is bulk density including rock and fluid, ρf is saturated fluid density and ρma is rock matrix density.

5.4.2 Effective Porosity

The following equation can calculate effective porosity:

$$\Phi eff = \Phi TOT - (\Phi sh * Vsh),$$

Where ΦTOT is total porosity, Φ_{sh} is porosity readings in the shale zone and V_{sh} is shale volume (Jelvegarfilband et al., 2022).

5.4.3 Density Porosity Cross Plots

Density neutron cross plots were created with Python scripts by using lasio, pandas, and Matplotlib libraries. For both wells, L-30 and B-41, density neutron cross plots were created and gamma ray is calibrated to get the shale and clay content information too. Three zones are interpreted in these cross plots, which are the shale zone with low values of neutron porosity and higher values of bulk density, the porous zone with clay having high values of neutron porosity and bulk density, and the gas zone with higher values of neutron porosity and lower values of bulk density (Rafei et al., 2021; Moosavi et al., 2024). Overall, for reservoirs of both wells, the clean and porous sand zone is not an ideal

zone for reservoirs, as higher values of gamma ray indicate the intercalation of clay/shale content in the sands, making this sand argillaceous, which is affecting the overall porosity and permeability of reservoirs in both wells.

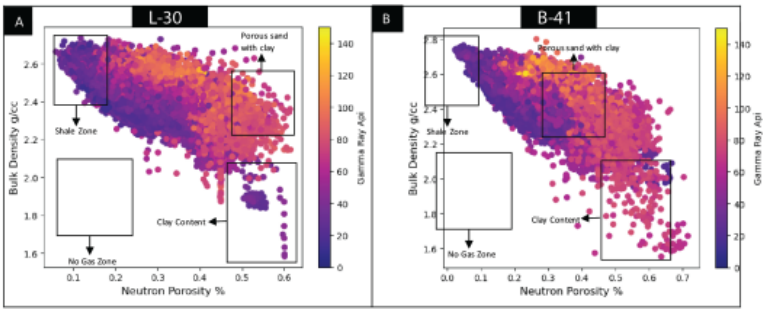

Figure 7. Bulk Density vs Porosity Cross Plots (A) Cross plot of L-30 well, (B) Cross plot of B-41(shale volume and porosity).

5.5 Estimation of Water Saturation

In reservoirs, the water saturation is calculated by following the Archie equation,

$$Sw = a / \varphi m \ * Rw / Rt,$$

where *Sw* is water saturation, *Rt* is resistivity, φ is porosity, *Rw* is water resistivity, and *m* and *a* are the cementation, saturation, and tortuosity factors, respectively (Moosavi et al., 2023).

Rw can be calculated by the following formula:

$$Rw = \varphi 2 * Rt$$

5.5 Petrophysical Results

This research estimates the total effective porosity using an advanced software program. The total porosity is calculated by using Bulk Density and Neutron porosity logs. According to Leverson's porosity classification, reservoir formations of B-41 and L-30 show fair effective and total porosity that ranges from 8-10% and 10-12%, respectively. Shale volume is calculated by equation 1, estimated shale volume is 37 to 44% and 23 to 32% for B-41 and L-30, respectively, which does not suggest a good reservoir. Both wells were declared dry, and the plug abounded. In conclusion the reservoir in B-41 (3000m to 3400m) is of poor quality, the content of volume of shale is high and assumed to be unfavorable for hydrocarbons to occur and the reservoir in L-30 (3400m-3600m) comprises of dominantly sandstone but intercalation of clay/shale matrix, however it shows a fair porosity but water saturation is high so that it is not favorable condition for hydrocarbon to accumulate.

5.6 Machine learning

In this paper, a crucial aspect of our methodology involves applying machine learning techniques to gain deeper insights into the geological attributes of the study area (Mehrabi et al., 2024). Specifically, we utilize Self-Organizing Maps (SOM) for data analysis. SOM is an unsupervised machine learning technique that uses a neural network to visualize and cluster high-dimensional data into a lower-dimensional representation (Mehrabi et al., 2025b). This involves SOM computation on a cross-plot incorporating 11, 18, and 26 Hz seismic frequencies, enabling us to identify and visualize intricate patterns and relationships within the seismic data. In this setup, porosity was assigned to the X-axis and frequency to the Y-axis, allowing the SOM algorithm to analyze the relationship between these two properties across the dataset. As the SOM processed the data, it

grouped similar input patterns into clusters, which are visually represented using different colors on the map. Lower frequencies (11 Hz) reveal deeper, large-scale structures; mid-range frequencies (18 Hz) capture medium-scale features like channels or faults; and higher frequencies (26 Hz) resolve thin beds and subtle facies changes near the wellbore. Additionally, we employ spectral decomposition techniques in conjunction with SOM for classification purposes. By combining SOM results with well log data, we were able to classify seismic patterns and correlate them with lithology, porosity, and fluid content at the well location. This approach enhanced our ability to identify reservoir zones and understand subsurface variability more effectively. The results of these machine learning-driven approaches are presented graphically in the figures below (Figures 8 and 9), offering a visual representation of our findings. These methodologies enrich our understanding of the subsurface geology and contribute significantly to the spatial analysis in our study of the Penobscot region in Nova Scotia, Canada.

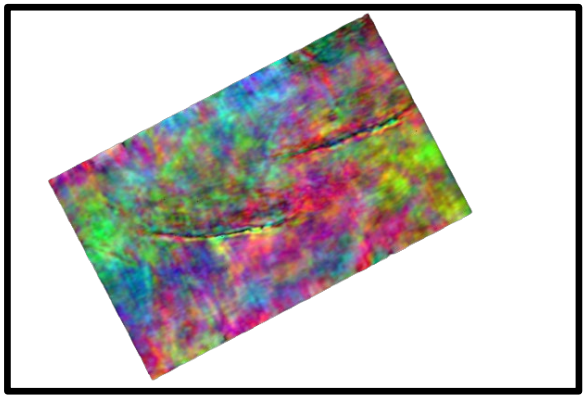

Figure 8. Spectral decomposition, classification by using SOM.

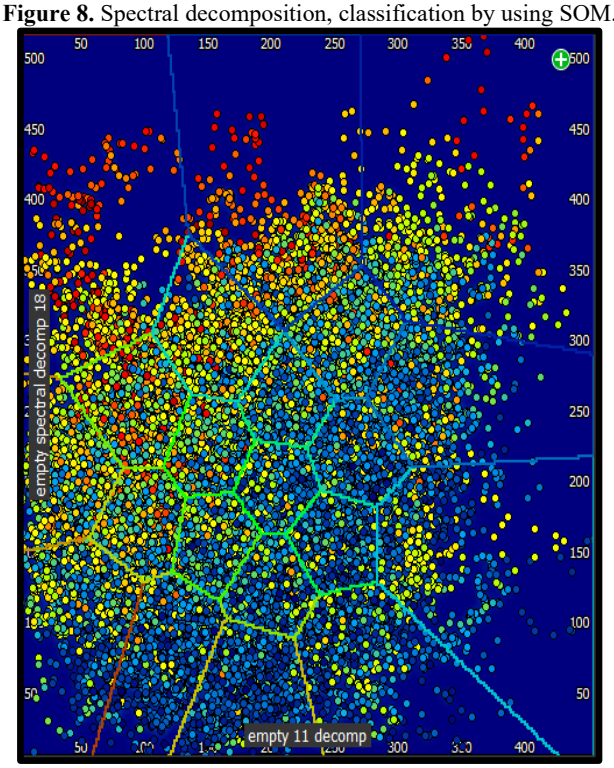

Figure 9. SOM computation on cross-plot between 11, 18 and 26 Hz.

6 Discussion

SOM machine learning technique was used for this research. SOM is an unsupervised learning algorithm that helps in clustering and visualizing high-dimensional data by reducing it into a 2D representation. Our input dataset included seismic attributes generated from spectral decomposition at multiple frequencies (11 Hz, 18 Hz, and 26 Hz). These frequencies were chosen to capture geological features at different scales, such as deep structures, medium-scale channels, and thin-bed reservoirs.

The first step involved feeding this high-dimensional seismic attribute dataset into the SOM algorithm. The SOM neural network, organized as a 2D grid of nodes, processed the data by allowing nodes to compete in representing input patterns. The winning node (Best Matching Unit) and its neighboring nodes were interactively adjusted to better match the input data based on similarity measures. Over successive iterations, the SOM organized the data into clusters that revealed hidden structures and relationships within the seismic volume.

By integrating SOM output with well data, we were able to interpret these clusters in terms of lithology, porosity, and fluid content. This machine learning approach allowed us to distinguish reservoir from non-reservoir zones, map geological features more accurately, and enhance the overall subsurface understanding, providing a data-driven and objective interpretation framework.

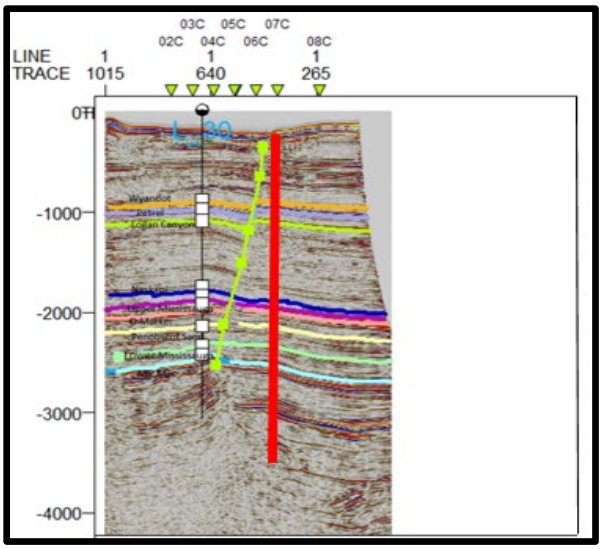

Figure 10. Illustrating the pseudo-well location delineated by a prominent red-colored line.

The spectral decomposition model in Figure 8 reveals two major faults that were not identifiable in conventional seismic data. By decomposing the seismic signal into multiple frequency components, spectral decomposition enhances the resolution and highlights subtle geological features. This technique allowed us to detect faults that would have remained hidden, thereby significantly improving the accuracy of our structural interpretation and contributing to a more reliable final result. No gas zone was identified based on density–neutron cross plots and wireline logs; the depth of B-41 and L30 ranges from 3000m to 3400 m and 3400m to 3600m, respectively. Lithological identification from cross plots indicates the presence of clay material with sands. High water saturation and high irreducible water might be the reason for low permeability and porosity in both reservoirs. The zone from 3430-3480 in well L-30 shows high resistivity values and indicates a hydrocarbon-bearing patch

with porosity approximately 10%, but this small patch is not enough for commercial extraction.

7 Conclusions

Our study region is located in the transitional zone between the Sable and Abenaki basins, providing a distinct geological environment for inquiry. It is situated within a passive margin. Four rifting periods have shaped this basin's complicated geological history over time. Basin modeling data further illuminate the subsurface dynamics, which in both wells show a constant reduction in porosity with increasing depth, highlighting the problems with reservoir quality.

Additionally, our petrophysical analysis reinforces these findings, emphasizing the prevalence of low porosity values within this geological domain. The integration of seismic attributes within our study also unveils the presence of two significant fault structures, further enriching our understanding of the geological intricacies in this region.

8 Novel / Recommendations

The L-30 well has been strategically positioned within the hanging wall of a prominent normal fault. In Figure 10, represented in red, our recommendation strongly advocates drilling a new well in the footwall of the fault. This strategic move is poised to optimize exploration efforts, offering the potential to unveil valuable geological insights at greater depths. By adjusting well locations slightly, we open up the possibility of identifying various trap types, including structural, stratigraphical, and combinations thereof. This adjustment could significantly enhance our exploration prospects and uncover new opportunities in this geological setting.

Acknowledgements

We would like to acknowledge the online database and Syed Sadaqat Ali for providing us with guidance and expertise for this work, respectively. We would also like to thank the Department of Earth Sciences, University of Sargodha, Sargodha, for its support.

References

Abid M., and Ali, S. H., 2024. Modified Approach To Calculate Brittleness Index In Shale Reservoirs, Socar Proceedings, 1 (2024) 003-009

Abid, M., Ba, J., Markus, U. I., Tariq, Z., Ali, S. H., 2025. Modified approach to estimate effective porosity using density and neutron logging data in conventional and unconventional reservoirs, Journal of Applied Geophysics, **233**, 105571.

Adim, A., Riahi, M., & Bagheri, M., 2018. Estimation of pore pressure by Eaton and Bowers methods using seismic and well survey data. Journal of Applied Geophysical Research, 4(2), 267-275.

Ahmed, T., Rehman, K., Hajana, M. I., Ahmed, S., Ali, S. H., Yasin, Q., 2025. A Reappraisal of Mesozoic-Cenozoic Sequence Stratigraphy in Offshore Indus Basin, Pakistan, Kuwait Journal of Science, Kuwait Journal of Science, **52**(1),100338.

Ali, A., Sheng-Chang, C., & Ali, S. H., 2022. Integration of Density-Based Spatial Clustering with Noise and Continuous Wavelet Transform for Feature Extraction from Seismic Data. Pure and Applied Geophysics, **179**(4), 1183-1195.

Ali, S.H., Poppelreiter, M.C., Shah, M.M., & Saw, B.B., 2018. Diagenetic understandings based on quantitative data, Miocene carbonate buildup, Offshore Sarawak, Malaysia. Petroleum and Coal, **60**(6), 1275-1282.

Bashir, Y., Morib, D. L., Babasafari,

A. A., Ali, S. H., Imran, Q. S., Siddiqui N. A., Karaman, A., 2024. Cohesive Approach for Determing Porosity and P-Impedance in Carbonate Rocks Using Sesimic Attributes and Inversion Analysis, Journal of Petroleum Exploration and Production Technology, 1-15.

Bashir, Y., Waheed, U. B., Ali, S. H., Karaman, A., İmren, C., 2024. Enhanced wave modeling & optimal plane-wave destruction (OPWD) method for diffraction separation and imaging, Computers and Geosciences, 105576.

Campbell, T. J., Richards, F. B., Silva, R. L., Wach, G., & Eliuk, L., 2015. Interpretation of the Penobscot 3D seismic volume using constrained sparse spike inversion, Sable sub-Basin, offshore Nova Scotia. Marine and Petroleum Geology, 68, 73-93.

Campbell, T. J., Richards, F. B., Silva, R. L., Wach, G., & Eliuk, L., 2015. Interpretation of the Penobscot 3D seismic volume using constrained sparse spike inversion, Sable sub-Basin, offshore Nova Scotia. Marine and Petroleum Geology, 68, 73-93.

Campbell, T., 2014. Seismic stratigraphy and attribute analysis of the Mesozoic and Cenozoic of the Penobscot Area, offshore Nova Scotia.

Campbell, T., 2018. Seismic Stratigraphy and Architecture of the Jurassic Abenaki Margin, at Cohasset-Migrant, and Potential for Distal Organic-Rich Facies.

Dentith, M., Enkin, R. J., Morris, W., Adams, C., & Bourne, B., 2020. Petrophysics and mineral exploration: a workflow for data analysis and a new interpretation framework. Geophysical Prospecting, 68(1-Cost-Effective and Innovative Mineral Exploration Solutions), 178-199.

Eliuk, L. S., 1978. The Abenaki Formation, Nova Scotia shelf, Canada—a depositional and diagenetic model for a Mesozoic carbonate platform. Bulletin of Canadian Petroleum Geology, 26(4), 424-514.

Fyffe, L. R., Johnson, S. C., & van Staal, C. R., 2011. A review of Proterozoic to Early Paleozoic lithotectonic terranes in New Brunswick, Canada and their tectonic evolution during Penobscot, Taconic, Salinic and Acadian orogenesis. Atlantic Geoscience, 47, 211-248.

Ghazi, S., Haroon, S. A., Shahzad, K., Ahmad, S., Baig, K. S., Waqas, M., & Ali, R. I., 2024. Structural Style and Its Implication to Hydrocarbon Potentiality of the Pishin Basin (Pakistan). Geotectonics, **58**(Suppl 1), S38-S53.

Gibling, M. R., Culshaw, N., Pascucci, V., Waldron, J. W. F., & Rygel, M. C., 2019. The Maritimes Basin of Atlantic Canada: Basin creation and destruction during the Paleozoic assembly of Pangea. In The sedimentary basins of the United States and Canada (pp. 267-314). Elsevier.

Jelvegarfilband, A., Riahi, M. A., & Bagheri, M., 2022. Prediction of Shale Volume and Water Saturation using Pre-Stack Seismic and Well-Log Data in an Oil Field. Iranian Journal of Oil and Gas Science and Technology, 11(1).

Kroner, U., Stephan, T., & Romer, R. L., 2022. Paleozoic orogenies and relative plate motions at the sutures of the Iapetus-Rheic Ocean.

Mehrabi, A. R., Bagheri, M., Nabi Bidhendi, M., Biniaz Delijani, E., & Behnood, M., 2025b. Enhancing Porosity Prediction Accuracy in Oil Reservoirs: Evaluating Hybrid Machine Learning Approaches Integrating Well Log and Core Data. Journal of the Earth and Space

Physics, 50(4).

Mehrabi, A., Bagheri, M., Bidhendi, M. N., Delijani, E. B., & Behnoud, M., 2024. Improved porosity estimation in complex carbonate reservoirs using hybrid CRNN deep learning model. Earth Science Informatics, 17(5), 4773-4790.

Mehrabi, A., Bagheri, M., Nabi Bidhendi, M., Biniaz Delijani, E., & Behnood, M., 2025a. Porosity estimation of carbonate reservoirs using a hybrid deep neural network model based on well data. Iranian Journal of Geophysics, 19(1), 143-164.

Mirza, M. Q., Bashir, Y., Ali, S. H., 2024. Application Of Probabilistic Seismic Hazard Assessment For Earthquake Hazard: Case Study Of Karachi City, Pakistan, Journal of Earth Sciences and Technology. **5**(1); 20–33.

Mixon, R. B., Pavlides, L., Powars, D. S., Froelich, A. J., Weems, R. E., Schindler, J. S., & Ward, L. W., 2000. Geologic map of the Fredericksburg 30'x 60'quadrangle, Virginia and Maryland (No. 2607). US Geological Survey.

Moosavi, N., Bagheri, M., & Nabi-Bidhendi, M., 2024. Hydrocarbon reservoir parameter estimation using a fuzzy Gaussian based SVR method. Bulletin of Geophysics & Oceanography (BGO), 65(4), 70.

Moosavi, N., Bagheri, M., Nabi-Bidhendi, M., & Heidari, R., 2023. Prediction of water saturation by fsvm using well logs in a gas field. Journal of the Earth & Space Physics, 48(4), 77.

Narayan, S., Sahoo, S. D., Kar, S., Pal, S. K., & Kangsabanik, S., 2023. Improved reservoir characterization by means of supervised machine learning and model-based seismic impedance inversion in the Penobscot field, Scotian Basin. Energy Geoscience, 100180.

Olutoki, J. O., Elsaadany, M., Siddiqui, N. A., Eahsanul Haque, AKM, Ali, S. H., Rashid, A., Akinyemi, O.D., 2024. Estimating petrophysical properties using Geostatistical inversion and data-driven extreme gradient boosting: A case study of late Eocene McKee formation, Taranaki Basin, New Zealand, Results in Engineering, **24**, 103494.

Omeru, T., Bankole, S. I., Jolly, B. A., Seyi, O. S., & Omojola, J. B., 2019. Assessment of the effect of mass-transport deposits on fault propagation in Penobscot area, offshore Nova Scotia. Geological Society, London, Special Publications, 477(1), 121-131.

Omeru, T., Bankole, S. I., Jolly, B. A., Seyi, O. S., & Omojola, J. B., 2019. Assessment of the effect of mass-transport deposits on fault propagation in Penobscot area, offshore Nova Scotia. Geological Society, London, Special Publications, 477(1), 121-131.

Pant, A., Ghosal, D., & Puryar, C., 2022. Imaging of a possible isolated carbonate build-up (ICB) in Penobscot Bay at anomalous low frequencies. Marine Geophysical Research, 43(1), 4.

Peace, A. L., Phethean, J. J., Jess, S., & Schiffer, C., 2024. Halokinetically Overprinted Tectonic Inversion of the Penobscot 3D Volume Offshore Nova Scotia, Canada. Pure and Applied Geophysics, 1-30.

Pe-Piper, G., & Piper, D. J., 2011. The impact of early cretaceous deformation on deposition in the passive-margin scotian basin, offshore Eastern Canada. Tectonics of sedimentary basins: Recent advances, 270-287.

Pharaoh, T., Haslam, R., Hough, E.,

Kirk, K., Leslie, G., Schofield, D., & Heafford, A., 2020. The Môn–Deemster–Ribblesdale fold–thrust belt, central UK: a concealed Variscan inversion belt located on weak Caledonian crust. Geological Society, London, Special Publications, 490(1), 153-176.

Pollock, J. C., Hibbard, J. P., & van Staal, C. R., 2012. A paleogeographical review of the peri-Gondwanan realm of the Appalachian orogen. Canadian Journal of Earth Sciences, 49(1), 259-288.

Rafei, M., Bagheri, M., & Nabi, B. M., 2021. Reservoir porosity modelling using support vector regression based on Gaussian kernel in an oil field of Iran. Journal of the Earth and Space Physics, 3: 421-432.

Robinson, P., Tucker, R. D., Bradley, D., Berry IV, H. N., & Osberg, P. H., 1998. Paleozoic orogens in New England, USA. Gff, 120(2), 119-148.

Saw, B. B., Poppelreiter, M., Vintaned, J. A. G., & Ali, S. H., 2017. Anatomy of an Isolated Carbonate Platform: Subis Limestone Outcrop, Early Miocene, Niah, Sarawak, Malaysia, 30th National Geological Conference, 9th- 10th October, 2017 At: Kuala Lumpur, Malaysia (Abstract Book).

Wach, G. D., & Brown, D. E., 2021. Petroleum exploration on the scotian margin. Geoconvention, 7.